ORIGINAL PAPER

A comparison of anodically grown CuO nanotube film and Cu₂O film as anodes for lithium ion batteries

J. Y. Xiang · J. P. Tu · X. H. Huang · Y. Z. Yang

Abstract CuO nanotube film and Cu₂O film were anodically grown on Cu substrates through direct oxidation and electrochemical anodic reduction, respectively. The microstructure and morphology of the films were characterized by X-ray diffraction (XRD) and scanning electron microscope (SEM). The obtained CuO is monoclinic crystallization, and the diameters of tubes are about 100–300 nm, while the as-prepared Cu₂O has a typical structure with a space group $Pn3m$ and consists of compact faceted crystals. As anodes for Li-ion batteries, the electrochemical properties of the nanostructured CuO and Cu₂O films were investigated by cyclic voltammogram and galvanostatic charge–discharge tests. An "apparent charge capacity" was introduced to describe the electrochemical performance. The initial apparent discharge capacity of the CuO and Cu₂O film electrode reached to 911 and 570 mAh/g, respectively. Although they exhibited large irreversible capacities attributed to the formation of solid electrolyte interface (SEI) during the first cycle, the CuO nanotube film and Cu₂O film had good cyclability and delivered the apparent capacity of 417 and 219 mAh/g after 30 cycles, respectively.

Keywords CuO · Cu₂O · Anodical growth · Film · Anode

Introduction

Nowadays, research efforts for anode materials of lithium ion batteries have been focused on the safety and capacity retention. Graphite and carbonaceous materials, which are commercially used, still have the drawbacks as low volume specific capacity and poor discharge performance at high charge/discharge rate. Although silicon-based, tin-based and other metal-based anodes have been reported as promising electrodes, the poor capacity retention limits their practical applications [1–6].

Recently, a novel mechanism of Li reactivity has been discovered in oxides of 3d transition metals (Fe, Co, Ni, and Cu), which differs from the classical Li intercalation and deintercalation or Li-alloying process but involves the formation and decomposition of Li₂O [7]. The investigation makes the research for novel anode materials, which deliver high electrochemical capacities and excellent cycle retention, true [8–11].

However, the powder oxides mentioned above still have some limitations in miniaturized batteries such as thin film Li-ion batteries. In this present work, CuO nanotube films and Cu₂O thin films were anodically grown on Cu substrates, through electrochemical anodic reduction and direct oxidation, respectively. The differences between structure, surface morphology, and electrochemical performance of the as-prepared CuO and Cu₂O films were discussed.

Experimental

Growth of CuO nanotube film

High-purity copper foils (99.99%) were used as substrate. After chemical polished in a mixed solution of acetic acid, nitric acid, phosphate acid, and distilled water, the clean copper foil, in which the diameter is 12 mm, is immersed into a mixed aqueous solution of NaOH (6 M) and (NH₄)₂S₂O₈ (1 M) as oxidant (the molar rate of NaOH and (NH₄)₂S₂O₈ is 20:1). The solution was set in a low-

J. Y. Xiang · J. P. Tu (✉) · X. H. Huang · Y. Z. Yang (✉)
Department of Materials Science and Engineering,
Zhejiang University,
Hangzhou 310027, China
e-mail: tujp@cmsce.zju.edu.cn
e-mail: yangyz@zju.edu.cn

temperature bath fixed at 0 °C for 4 h to gain more ordered $Cu(OH)_2$ nanotubes [12], then at 25 °C for about 8 h to obtain more tubes. After that, the copper foil specimen were taken out of the solution, washed them with distilled water and ethanol, and dried in the air.

The corresponding $Cu(OH)_2$ film precursors on Cu foils were put in a crucible boat, which was set in the quartz tube in a furnace in flowing Ar. The temperature of the furnace was set at 60 °C for 2 h first, and then at 120 °C for 4 h, and last at 180 °C for 6 h. The CuO film on copper was obtained until the furnace was naturally cooled to room temperature.

Growth of Cu_2O thin film

Electrochemical growth of Cu_2O film was accomplished by using a conventional three-electrode cell, carried out in a galvanostatic mode. After the same chemical polished process as above, the copper foil substrate (12 mm in diameter) was used as working electrode, a platinum sheet as counter-electrode, and saturated calomel electrode (SCE) as reference electrode. The electrolytic bath was an aqueous solution of sodium hydroxide (4 M), which was kept at the temperature of 65 °C. The current density applied on the copper substrate was set at 0.005 A/cm^2.

Characterization

X-ray diffraction (XRD Rigaku D/max-rA, Cu Kα) was used to identify the crystalline phase of the as-prepared films on Cu foils. The surface morphologies of the films were observed using a field-emission scanning electron microscopy (FSEM SIRION JY/T010–1996).

The electrochemical measurements were performed using a coin-type half cell, as assembled under argon
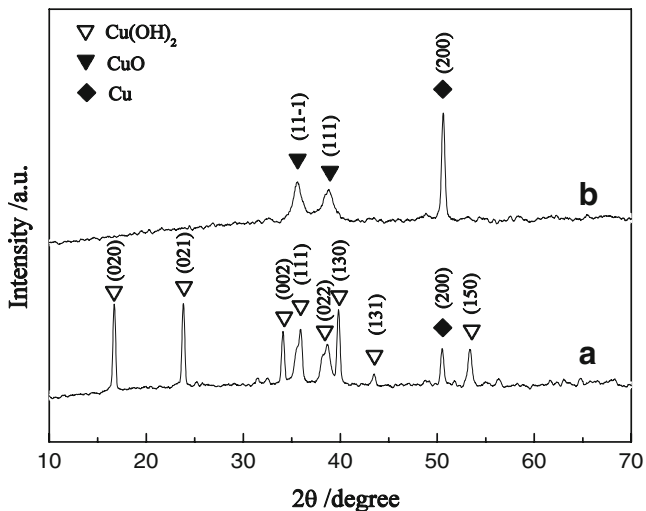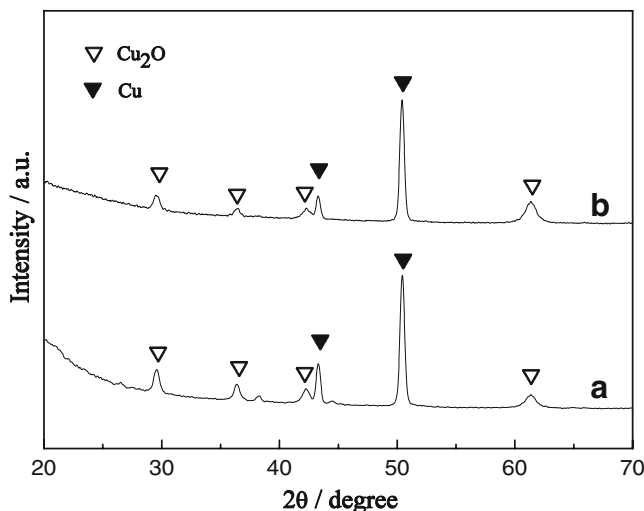
Fig. 2 XRD patterns of the Cu_2O films grown at the current density of 0.005 A/cm^2 for **a** 90 s, **b** 300 s

atmosphere. The as-prepared thin-film on copper foil was used as working electrode, the metallic lithium foil as counter-electrode, 1 M $LiPF_6$ in ethylene carbonate (EC)–dimethyl carbonate (DME; 1:1 in volume) as the electrolyte solution, and a polypropylene (PP) microporous film (Cellgard 2300) as the separator. The galvanostatic charge–discharge tests were conducted at a current density of 0.02 mA/cm^2 between 0.2 and 2.5 V vs Li/Li$^+$, on a PCBT-138-8D-A battery program-control test system.

Results and discussion

Figure 1 shows the XRD patterns of the films obtained by electrochemical anodic reduction and post-treatment on Cu substrate. The precursor film before thermal treatment has typical crystallized $Cu(OH)_2$ of orthorhombic structure except for the peak marked with (200), which can be
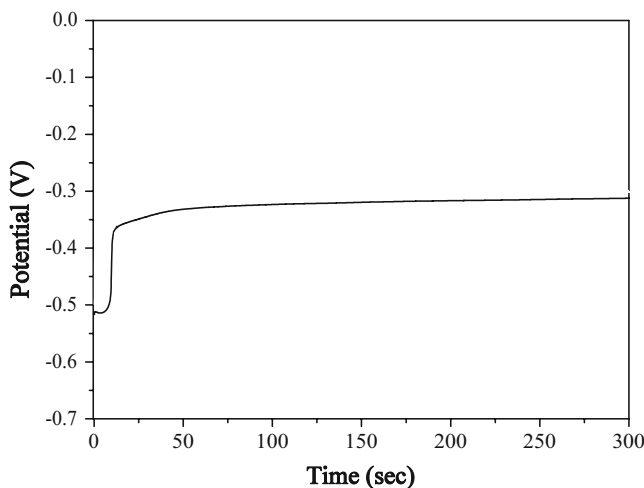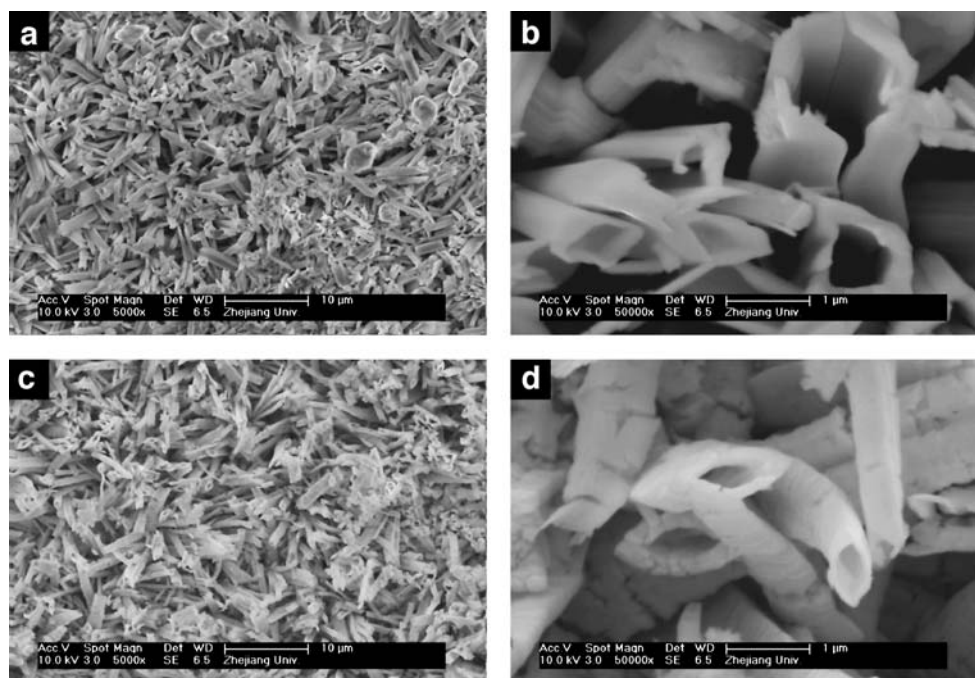
Fig. 1 XRD patterns of **a** $Cu(OH)_2$ precursor film, **b** CuO film obtained by heat treatment in Ar atmosphere

Fig. 3 The potential variation versus growth time at the current density of 0.005 A/cm^2

Fig. 4 SEM images of **a** and **b** Cu(OH)$_2$ precursor film; **c** and **d** CuO film obtained by heat treatment in Ar atmosphere

indexed to Cu substrate. However, the peaks that indexed to Cu(OH)$_2$ disappear in the film after heat treatment under Ar atmosphere; the peaks marked with (11–1) and (111) appear, which can be readily indexed to crystalline monoclinic structure CuO with a lattice constant of a= 4.688 Å, b=3.423 Å, c=5.132 Å.

Figure 2 presents the XRD patterns of the films electrochemically grown on Cu substrate at the current density of 0.005 A/cm^2. The as-prepared films have a typical structure with a space group $Pn3m$. Besides the Cu peaks originated from the substrate, all the diffraction peaks could be indexed according to cubic phase Cu$_2$O, whether grown for 90 or 300 s. The electrochemical process could be expressed as Eq. 1 [13].
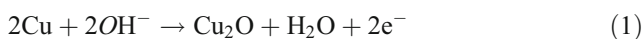
$$2Cu + 2OH^- \rightarrow Cu_2O + H_2O + 2e^- \tag{1}$$

Figure 3 shows the potential variation vs growth time at the current density of 0.005 A/cm^2. The shape of the film growth curve can clearly indicate the nucleation–growth mechanism [14]. At the beginning, the potential vs SCE is a relative negative. It indicates the formation of Cu$_2$O on the bare substrate. Seconds later, the potential becomes less negative and stable, which is at around −0.3 V (vs SCE), exactly in the potential range where cuprous oxide forming in the Pourbaix diagram for the system Cu–H$_2$O [15, 16]. Therefore, it can be explained that further growth of the Cu$_2$O layer is facilitated after a certain number of nuclei are formed.

The morphologies of the precursor Cu(OH)$_2$ and the final CuO film are shown in Fig. 4. Both the films exhibit the tube-like morphology, but there are still some cauliflower-like groups in the Cu(OH)$_2$ precursor film, which is not so uniform as the CuO film treated in flowing Ar. Compared with the diameters of Cu(OH)$_2$ tubes, which are about 400−600 nm, the CuO tubes have smaller diameters of 100−300 nm. The morphology of nanotube is favorable for the electrochemical process. Appropriate specific surface area can provide more contact area between lithium ions and active anode material CuO, which is favorable in increasing the specific capacity and improving the efficiency of discharge and charge process.

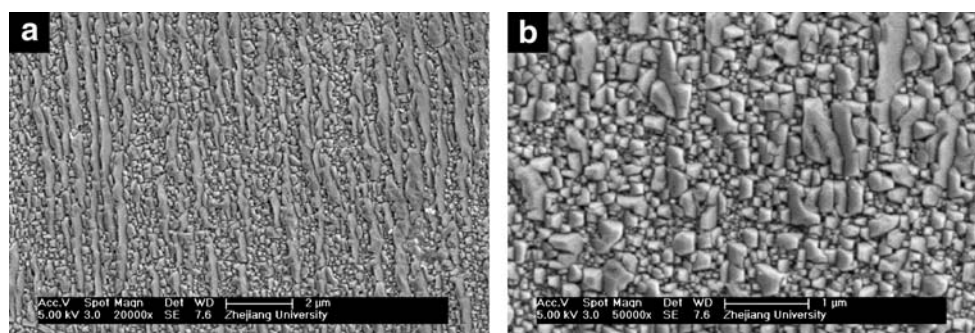**Fig. 5** SEM images of the Cu$_2$O films grown at a current density of 0.005 A/cm^2 for 90 s

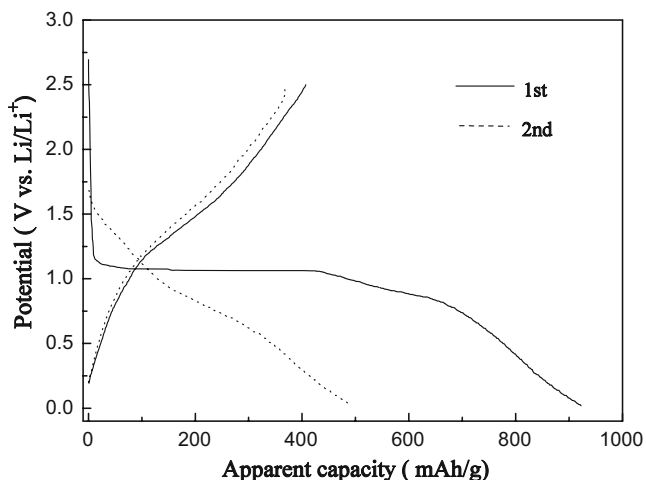Figure 5 shows the typical morphologies of the as-prepared Cu_2O films. The Cu_2O films consist of faceted crystals, which are 100−500 nm in sizes, and compact well with each other.

The films anodically grown on Cu substrate are too thin to evaluate the amount of active materials accurately by conventional mass measuring method. Particular estimate methods were used to calculate the mass of active materials. To obtain the mass of CuO grown on Cu substrate, a piece of high-purity copper foil with diameter of 36 mm, which was as three times large as 12 mm, was used as the substrate. The increasing mass of the foil after anodic oxidation could be easily measured through a balance, which weigh nine times than the mass grown on the foil with the diameter of 12 mm. Hence, the amount of CuO active material could be approximately evaluated.

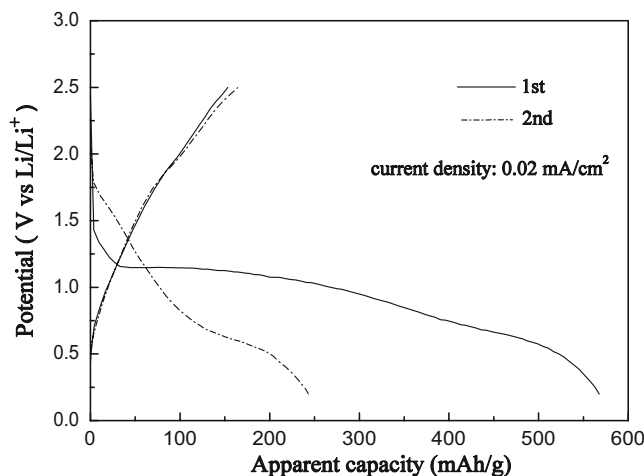The quantity of Cu_2O grown on the Cu substrate was determined by both the applied current density and growth time. Hence, a method of coulometric determination was used to calculate the mass of Cu_2O on Cu substrate. There would be 0.34 mg/cm^2 of Cu_2O grown during the anodic oxidation process at the current density of 0.005 A/cm^2 for 90 s.

As the amount of active materials calculated by the methods above is theoretic, not as conventional coin cell experiments where material is weighed in, "apparent charge capacity" is used to evaluate the electrochemical performances of CuO and Cu_2O thin films in this work.

Figures 6 and 7 show the first and second galvanostatic charge–discharge curves for the CuO nanotube film and Cu_2O film on copper foil ranging from 0.2 to 2.5 V, respectively. There are both two long plateaus during the initial discharge in the two figures, one is at the potential of about 1.0 V, the other is around 0.7 V, which correspond with the electrode reaction and the decomposition of solid electrolyte interface (SEI) [17], respectively. The electrode
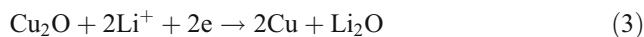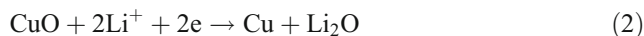

Fig. 7 The first and second cycle curves of the Cu_2O film grown on copper foil at the current density of 0.005 A/cm^2 for 90 s ranging from 0.2 to 2.5 V

reactions of CuO nanotube film and Cu_2O film during charge–discharge process are expressed in Eqs. 2 and 3 as below [17].

$$CuO + 2Li^+ + 2e \rightarrow Cu + Li_2O \tag{2}$$

$$Cu_2O + 2Li^+ + 2e \rightarrow 2Cu + Li_2O \tag{3}$$

The CuO nanotube film delivers the apparent initial discharge capacity of 911 mAh/g, although it exhibits a large irreversible capacity attributed to the formation of SEI during the first cycle. During the second discharge–charge process, the two plateaus appear at the potentials of about 1.2 and 0.7 V, although they are not so distinct as which appear in the first discharge, while the Cu_2O film delivered the apparent initial discharge capacity of about 570 mAh/g.

Fig. 6 The galvanostatic charge–discharge curves for CuO nanotube film on copper foil within the first and second cycles ranging from 0.2 to 2.5 V
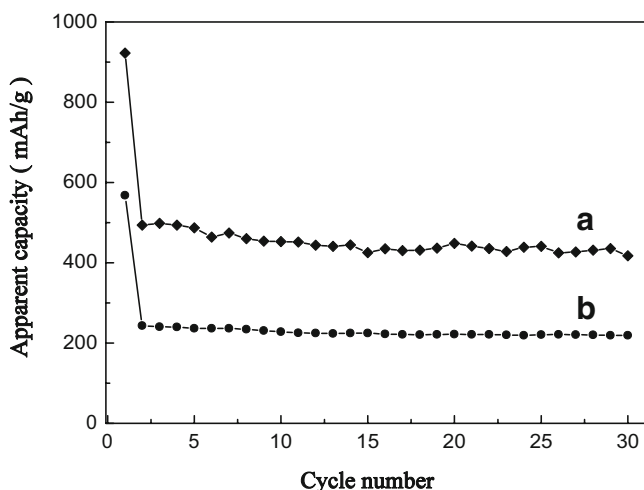

Fig. 8 Cycling performance of a CuO nanotube film, b Cu_2O thin film anodes on copper foil at the current density of 0.02 mA/cm^2

In general, the Li_2O formed in the first discharge process is regarded as unable to be decomposed by electrochemical method. The presence of Cu nanoparticles [17], which have the high surface activity, can enhance the reactivity of Li_2O decomposition and improve the reversibility of Li_2O back to Li in the recharge process. The irreversible capacity between first and second cycle is caused by Li-driven irreversible electrochemical reaction and lithium-driven irreversible structure or texture modification.

The cycling performances of CuO nanotube film and Cu_2O thin film on copper substrate are shown in Fig. 8. For each film anode, there is a large irreversible capacity loss in the first discharge–charge process, which is mainly attributed to the formation of SEI during the first cycle. However, in the remaining cycles, the CuO nanotube film and Cu_2O thin film exhibit good cyclability and delivers the apparent discharge capacity as high as 417 and 219 mAh/g after 30 cycles, respectively.

Conclusion

CuO nanotube film and typical cubic phase Cu_2O thin films were successfully synthesized through electrochemical anodic reduction and direct anodic oxidation on Cu substrates. The obtained CuO was monoclinic crystallization, and the CuO nanotube were 100−300 nm in diameters. The tube structure had an advantageous effect on the electrochemical performance, which was attributed to the increase of contact surface between the active electrode material and lithium ions. The cubic phase Cu_2O thin films consists of compact faceted crystals. In comparison with the electrochemical performances, the CuO nanotube film and Cu_2O thin film delivered the apparent initial discharge capacity of 911 and 570 mAh/g, respectively. There were large first capacity losses in both two films attributed to the formation of SEI. But in the remaining cycles, the CuO nanotube film and Cu_2O thin film could exhibited good cyclability, and delivered the apparent capacity as high as 417 and 219 mAh/g, respectively.

References

1. Guy S, Philippe B, Michel B (2004) J Power Sources 127:65
2. Lee YT, Yoon CS, Sun YK (2005) J Power Sources 139:230
3. Yang Z, Wu H (2001) Solid State Ion 143:173
4. Wang GX, Ahn JH, Yao J, Bewlay S, Liu HK (2004) Electrochem Commun 6:689
5. Shi DQ, Tu JP, Yuan YF, Wu HM, Li Y, Zhao XB (2006) Electrochem Commun 8:1610
6. Idota Y, Kubota T, Mastufuji A, Maekawa Y, Miyasaka T (1997) Science 276:1395
7. Poizot P, Laruelle S, Grugeon S, Dupont L, Tarascon JM (2000) Nature 407:496
8. Wang GX, Chen Y, Konstantinov K, Lindsay M, Liu HK, Dou SX (2002) J Power Sources 109:142
9. Badway F, Plitz I, Grugeon S, Laruelle S, Dollé M, Gozdz AS, Tarascon JM (2002) Electrochem Solid State Lett 4:A115
10. Larcher D, Masquelier M, Bonnin CD, Chabre Y, Masson V, Leriche JB, Tarascon JM (2003) J Electrochem Soc 150:A133
11. Obrovac MN, Dunlap RA, Sanderson RJ, Dahn JR (2001) J Electrochem Soc 148:A576
12. Zhang WX, Ding SX, Yang ZH, Liu AP, Qian YT, Tang SP, Yang SH (2006) J Cryst Growth 291:479
13. Biestek T, Weber J (1976) Electrolytic and chemical conversion coating. Portcullis Press, London
14. Jongh PE, Vanmaekelbergh D, Kelly JJ (1999) Chem Mater 11:3512
15. Pourbaix M (1974) Atlas of electrochemical equilibria in aqueous solutions. National Association of Corrosion Engineers, Houston
16. Pourbaix M (1973) Lectures on electrochemical corrision. Plenum Press, New York
17. Grugeon S, Laruelle S, Herrera-Urbina R, Dupont L, Poizot P, Tarascon JM (2001) J Electrochem Soc 148:A285